Fluid Depletion in Shear Bands

Roman Mani,[1,*] Dirk Kadau,[1] Dani Or,[2] and Hans J. Herrmann[1,3]

[1]*Computational Physics, IfB, ETH-Hönggerberg, Wolfgang-Pauli-Strasse 27, 8093 Zürich, Switzerland*
[2]*Institut für Terrestrische Oekosysteme, ETH-Zentrum, Universitätsstrasse 16, 8092 Zürich, Switzerland*
[3]*Departamento de Física, Universidade Federal do Ceará, Fortaleza, Ceará 60451-970, Brazil*

(Received 4 May 2012; published 10 December 2012)

How does pore liquid reconfigure within shear bands in wet granular media? Conventional wisdom predicts that liquid is drawn into dilating granular media. We, however, find a depletion of liquid in shear bands despite increased porosity due to dilatancy. This apparent paradox is resolved by a microscale model for liquid transport at low liquid contents induced by rupture and reconfiguration of individual liquid bridges. Measured liquid content profiles show macroscopic depletion bands similar to results of numerical simulations. We derive a modified diffusion description for rupture-induced liquid migration.

DOI: 10.1103/PhysRevLett.109.248001 PACS numbers: 45.70.−n, 47.55.nk, 83.50.Xa

Is interstitial pore liquid driven away or drawn into shear bands during deformation of granular matter? In fully saturated granular materials it is known that liquid is sucked into dilating shear bands with increase in porosity [1–4] since air is precluded from entering the dilated shear band pore volume. In unsaturated granular media, however, at low liquid contents with continuous air phase it is unclear if the liquid content increases or decreases. In this work we show that in the pendular regime where only capillary bridges are present, a liquid migration pattern opposite to that observed for saturated media develops. Despite increase in porosity in the shear band, liquid content consistently decreases. Liquid migration is of tremendous importance to the stability properties of soil structures [5,6]. Partially saturated soils may be considered as brittle due to the collapse of menisci in the failure plane [7]. Furthermore, granular materials generally lose strength with decreasing liquid content [8]. On the other hand, liquid accumulation in soil pores may cause a dramatic decrease in strength leading, e.g., to landslides or soil collapses [5,9]. Moreover, liquid migration is also of great interest in a variety of other situations in powder technology or pharmaceutical applications where grains are mixed with liquid, e.g., in spray coating of tablets [10]. It was reported that in partially saturated soils, liquid migrates away from the shear plane due to the formation of microcracks and increasing connectivity near the failure plane [11]. On the grain level, however, first experimental investigations on partially saturated soils using nondestructive techniques have been performed only recently [12] and the authors did not measure the liquid content. In this Letter, we experimentally measure fluid depletion patterns in shear bands using a split bottom shear cell [13] and propose a novel model with capillary bridges capable of reproducing the experimental results. We show how the inclusion of flow dynamics between individual liquid structures leads to the observed fluid depletion and explain our findings within a diffusive description of the flow dynamics.

Experiment.—To investigate liquid transport in regions of strain localization, it is desirable to realize a stable shear band at a fixed position. The circular split bottom cell [13] used in our experiments satisfies this requirement. Our split bottom cell, sketched in Fig. 1, consists of two circular L shapes where the inner part is made of a rotating cylinder at constant velocity (radius 10 cm) and the outer part is fixed. The distance from the symmetry axis of the cell to the outer wall is 18 and 15 cm to the slit where the L shapes join. We define a coordinate z along the axis of the inner cylinder. Glass beads (from Sigmund Lindner, SiLi beads type S) with radii $R = 0.85 \pm 0.075$ mm were used. In order to measure the liquid distribution in the bulk of the sample, we used a UV glue (from Norland products, NOA 61) that hardens after irradiation with ultraviolet light. In the liquid state it has a surface tension Γ of 40 mN/m, which is close to that of water, a viscosity η of 300 mPa s, and from electron microscopy the contact angle on glass was estimated to be less than 10°. The glue and beads were thoroughly stirred in a glass container until the glue appeared homogeneously distributed. The shear cell was then filled up to 1.5 cm. Too large filling heights delay the hardening of the glue. Initially, not all bridges have the same volume, but the spatially averaged liquid distribution is homogenous. After shearing, the glue is immediately hardened, such that subsequent measurements of the liquid content are possible with virtually no time delay.

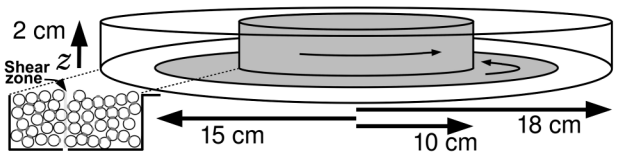

FIG. 1. The circular split bottom shear cell consists of a rotating inner part (shaded in gray) as well as a fixed outer part (white) separated by a thin slit. The gray cylinder and ring rotate at the same angular velocity.

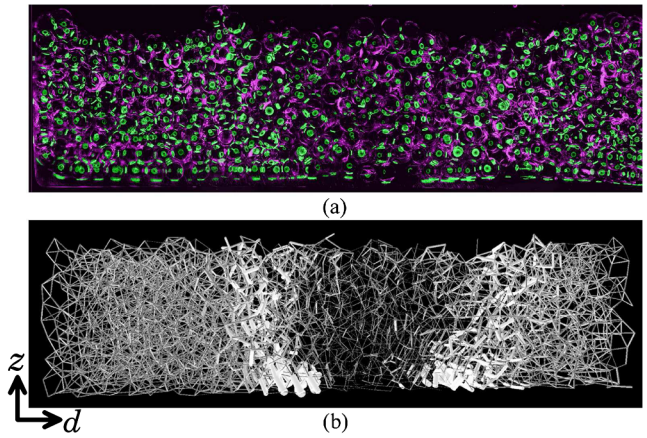

FIG. 2 (color online). (a) A slice perpendicular to the shear band after a shear displacement of 8 turns. Liquid [artificially highlighted in light gray (green)] has migrated away from the shear band and is accumulated along the edges of the shear zone. The beads were artificially marked dark gray (purple). (b) A slice perpendicular to the shear band as obtained in simulations. We only show the capillary bridges represented by lines of width and brightness proportional to their volume. The width of both images is 60 mm. The coordinate d points from the outer wall towards the symmetry axis.

For visualization we mixed the UV glue with a fluorescent dye, and in order to cut the sample into slices after hardening, we filled all remaining pore space with a clear and colorless epoxy resin and checked that the liquid bridges remain in their original state. The rotation speed was fixed to $\omega = 2\pi/600\ \mathrm{s}^{-1}$, the overall shear displacement was 8 turns, and the liquid content was 1%, which is the liquid volume divided by the volume of the sample. Figure 2(a) shows a slice along a plane perpendicular to the shear band. Indeed, liquid is driven out of the shear band and is accumulated along the edges. The thin blue curve in Fig. 3 shows the liquid content obtained experimentally as a function of the distance d from the outer fixed wall averaged over bridges having a height larger than $z = 3.4$ mm.

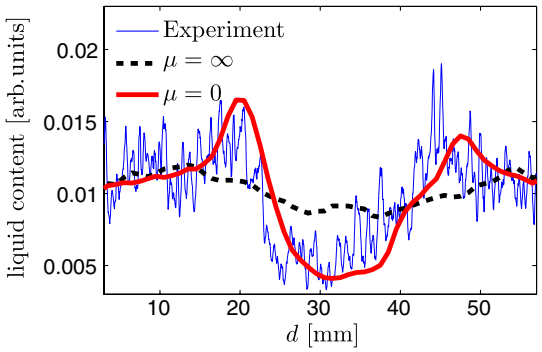

FIG. 3 (color online). The liquid content from simulation ($\mu = 0$) and experiment agree well. A depletion in humidity is found inside the shear band after 8 turns. The dashed line ($\mu = \infty$) is equivalent to a suction controlled model.

Because of strong noise, we were limited to averaging only over the largest possible z range. Additionally, the data were smoothed using a running average filter of window size 0.28 mm. To determine the liquid content, we counted the amount of pixels belonging to a liquid bridge in the images taken by an optical microscope and averaged over 8 slices. We also found that the Fourier spectrum of the unsmoothed data is exponentially decaying for large enough frequencies not revealing any further hidden characteristic length scales.

Numerical model.—To understand the redistribution of liquid in sheared granular flows, we develop a model with capillary bridges including liquid flow dynamics. We use contact dynamics [14,15] with cohesive forces due to capillary bridges and Coulombian friction to model rigid spherical particles with radii uniformly distributed between 0.775 and 0.925 mm. Simple models for cohesive forces are well established in contact dynamics [16–18]. We use empirical formulas for the capillary force which have been suggested by Willett *et al.* [19].

The grains are characterized by a certain roughness in which liquid may accumulate and form a wetting layer. As soon as liquid layers coating the particles are brought into contact, a capillary bridge having a small volume is formed [20,21]. Experimental observations reveal that small bridges grow in favor of larger ones due to liquid fluxes driven by Laplace pressure differences either through the vapor phase, which is presently not the case, or through thin wetting layers on the beads [8], which we call minimal wetting layers. The associated flow resistance for thin films is essentially independent of the film thickness [22], such that the dynamics can be modeled by taking the flux between two bridges as proportional to the pressure difference. Since the volume of the minimal wetting layers on the beads is small compared to the volume of the bridges, we do not consider the volume of the minimal films explicitly. Instead, whenever two beads come into contact, we initialize the liquid bridge with a small volume which is sucked out of the neighboring bridges. Once a liquid bridge has formed, it becomes part of the contact network in which the bridge volumes V_i are constantly updated according to $\dot{V}_i = \mu \sum_j (P_j - P_i)$, where P_i is the pressure in contact i and the sum runs over all neighbors j of contact i, and $\mu \propto \eta^{-1}$ is the inverse flow resistance of the film which is a model parameter. When the separation between two grains exceeds the distance $V_i^{1/3}$, the liquid bridge ruptures [19] and the liquid is sucked back onto the grains fast [20]. In that case, we equally distribute the liquid among the two particles. Since the film swells (the volume of the film becomes V_f) and the flow resistance drops, we assume that the liquid is instantaneously sucked into all neighboring bridges regardless of the choice of μ. Each bridge receives an amount of liquid $\Delta V_i = A(P_f - P_i)/L_i$, where $P_f = \Gamma/R$ is the pressure in the film, L_i is the distance from the rupture point to the bridge i, and A is a

normalization factor such that $\sum_i \Delta V_i = V_f$. The flow dynamics in our model is asymmetric: The time scale for liquid redistribution after bridge rupture is infinitely short while the time scale for equilibration of liquid bridges is controlled by μ. For $\mu \to \infty$, our model is equivalent to a suction controlled model where the Laplace pressures of all liquid bridges are equal. Traditionally, slow deformations, e.g., in geotechnics, are usually studied by means of suction controlled models [23]; however, our model is also applicable to faster grain movements as long as the shearing velocity is below the capillary velocity Γ/η since, then, the assumption of instantaneous liquid redistribution upon bridge rupture is no longer justified. When this requirement is met, the dynamics is fully controlled by μ; i.e., decreasing the shearing velocity or the viscosity in experiments requires increasing μ in simulations.

Using this model we simulate shear flow in the circular split bottom shear cell with the same dimensions as in the experiment without rough boundary conditions. However, since the system is rotationally invariant with respect to the z axis, we only consider a sector of the cell with arc length $\vartheta = 0.0873$. We use periodic boundary conditions in the ϕ direction, where in cylindrical coordinates, ϕ is the angular coordinate. Note that the cylinder walls as well as the two bottom rings are considered to be completely hydrophobic. In our experiments, the spatially averaged liquid concentration is constant before shearing; thus, all bridges are initialized with the same amount of liquid. In steady state, for $\mu = \infty$ (traditional model), the liquid content shown in Fig. 3 (black dashed line) was found to be proportional to the number of contacts only, which is slightly decreased in the shear band. The depletion observed in experiments (thin blue curve) is, however, significantly stronger.

For $\mu = 0$, the liquid distribution after the same shear displacement as in experiments is in good agreement with the experimental data. The data were averaged over 5 independent runs and smoothed using a running average filter of window size 1 mm. We also show a snapshot of the capillary bridge network for $\mu = 0$ in Fig. 2(b). Why could the flow resistance μ^{-1} be set so large in the simulation? The equilibration time t_0 of liquid bridges is expected to scale as $\eta R^2/\Gamma$ [20]. For water and glass beads of 0.5 mm diameter, t_0 is of the order of 1–5 min [8,24,25]. Since η/Γ for the glue is 562 times larger than for water, t_0 for our system is at least 9 h, which is very large compared to the contact time of beads in the shear band. Therefore, the liquid bridges are not equilibrated by liquid fluxes through minimal wetting layers. However, liquid from thick films arising via bridge rupture is still expected to fully drain since the capillary velocity is well above the shearing velocity v. Consequently, flow takes place mainly via bridge rupture events leading to liquid fluxes pointing away from the shear zone such that not only the coordination number but also the average bridge volume is reduced inside the shear band. The depletion should become apparent for all wetting liquids when keeping $v\eta/\Gamma$ fixed, also for water which is of importance for most environmental applications. Lowering v or η/Γ would lead to a smaller depletion but could be controlled by μ until the suction controlled model ($\mu = \infty$) is recovered.

Diffusive description.—We now explain the occurrence of the liquid depletion in terms of a theoretical model. For simplicity, we first consider a one-dimensional shear rate profile which, e.g., occurs in plane shear flows between two parallel walls separated by some distance along the z direction. We divide the plane shear geometry into slices of thickness h along the z axis. Since μ is small in our experimental system the main transport happens via rupture of individual capillary bridges. If pressure differences are not too large, there is on average an isotropic transport of liquid away from the rupture point which is proportional to the volume of the ruptured bridge. Thus, the amount of liquid leaving a slice of our model plane shear geometry during a time interval Δt is proportional to the bridge rupture rate and to the average bridge volume in the slice. The same holds for the neighboring slices $i-1$ and $i+1$, such that the total change of liquid in slice i can be written as

$$Q^i(t+\Delta t) - Q^i(t) = \frac{\chi \Delta t}{2}(B^{i-1}Q_b^{i-1} + B^{i+1}Q_b^{i+1} - 2B^iQ_b^i), \tag{1}$$

where Q^i is the total amount of liquid, B^i the bridge rupture rate, Q_b^i the average bridge volume in slice i, and χ is a geometrical proportionality factor which measures the average amount of liquid leaving a slice after each rupture event. The bridge creation rate is neglected since the initial volume of a liquid bridge is small. Thus, the flux induced by bridge rupture is large compared to that by bridge creation. The bridge rupture rate is expected to be proportional to the shear rate $\dot\gamma$ and to the number of contacts N. After dividing both sides by N and assuming that N is slowly varying with z, we arrive at the following continuum equation (for more details, see the Supplemental Material [26])

$$\dot Q_b = C\frac{\partial^2}{\partial z^2}(\dot\gamma Q_b) \tag{2}$$

on length scales larger than h, and $\Delta t \to 0$. Here, C is a constant and Q_b is the average bridge volume. The particles themselves behave diffusively in plane shear flow [27]. Therefore, the liquid bridges also diffuse in space, giving rise to an additional diffusive contribution $\dot Q_b \sim (\dot\gamma Q_b)''$ to Eq. (2), which could be lumped into the constant C.

A nice feature of Eq. (2) is that, for constant $\dot\gamma$, the liquid spreads diffusively as observed in a variety of industrial processes [10]. However, Eq. (2) is not an ordinary diffusion equation as $\dot\gamma$ is not a global constant. Indeed, the equation predicts that even homogeneous liquid distributions will

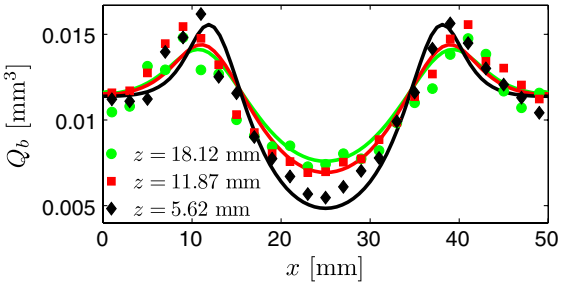

FIG. 4 (color online). The average bridge volume Q_b in the linear split bottom shear cell is plotted for different z as a function of x after a shear displacement of 8 m. The data from simulations (symbols) agree well with the numerical solution (lines) of Eq. (2).

change if the second derivative of the shear rate profile $\dot{\gamma}''$ with respect to z is large. We now address the liquid depletion pattern observed: The shear rate profile in split bottom shear cell geometries is Gaussian [13,28] and its width $W(z)$ increases as a function of z. Therefore, at fixed z, $\dot{\gamma}''$ is smallest and negative in the center of the shear band, which causes a liquid content drop due to fluxes away from the center induced by rupture of individual bridges. However, it is largest and positive at the edges, which explains the accumulation of liquid along the edges of the shear band.

To validate the proposed model, we simulate the simpler linear split bottom shear cell [28], which consists of two straight L shapes sliding past each other, and we compare to the numerical solution of Eq. (2). We now use Cartesian coordinates where the x direction is perpendicular and the y direction is parallel to the slit, and the z direction is perpendicular to the bottom plates. To ensure a homogenous sample, we add a frictionless top plate on which a force is exerted to confine the grains in the container and we switch off gravity as well as cohesion. The dimensions of the system are now $L_x = 50$ mm, $L_y = 18$ mm, and $L_z \sim 19$ mm. The bead radii are uniformly distributed between 0.735 and 0.925 mm and we use rough boundary conditions.

Our system is effectively two dimensional, since it depends on both x and z. Thus, we generalize Eq. (2) to $\dot{Q} = C \triangle (|\dot{\gamma}|Q)$, where $|\dot{\gamma}|$ is the second invariant of the shear rate tensor [29]. This equation is solved over the domain $z > 0.625$ mm by using von Neumann boundary conditions, where the component normal to the boundaries at $z = 0.625, 19$ mm and $x = 0, 50$ mm of $\nabla(|\dot{\gamma}|Q)$ is set to zero, using the same initial condition and shear rate as in the simulation and $C = 0.0675$ mm^2. Figure 4 shows the simulation results for Q_b as a function of x and different z (symbols), which are in good agreement with the numerical solution of the previous equation (lines). Only for small z, the results agree less well. We attribute this to the fact that the shear rate near the bottom rings varies on small length scales, which is not resolved in the averages of the simulations. Note that, although the system is mechanically in steady state, the liquid distribution still changes over longer time scales until $\nabla(|\dot{\gamma}|Q)$ is spatially constant.

Conclusion.—We found that liquid content decreases within unsaturated shear bands experimentally and in simulations. A simple model for liquid redistribution explains this discovery while purely suction controlled models fail. We derived a modified diffusion equation describing bridge rupture-induced liquid migration within the system. Our work shows that knowing how liquid is redistributed due to shear is crucial for prolonged simulations and experiments in the field of wet granular matter where liquid depletion may induce noticeable shear softening. The equilibration time is set by the fluid properties and grain sizes; thus, keeping the ratio between the equilibration and the contact time fixed is sufficient to obtain unchanged results making our theory applicable to various fluids and grain sizes and hence to a broad range of scientific areas, e.g., to soil science and powder technology up to a liquid content of 2.4% [8] where bridge coalescence sets in.

We would like to thank Martin Brinkmann for helpful discussions. We greatly acknowledge the provision of a look-up table allowing the determination of the Laplace pressure by Ciro Semprebon as well as technical support by Daniel Breitenstein and Gabriele Peschke. We thank the Deutsche Forschungsgemeinschaft (DFG) for financial support through Grant No. HE 2732/11-1.

*manir@ethz.ch

[1] P. Y. Hicher, H. Wahyudi, and D. Tessier, Comput. Geotechnics **16**, 205 (1994).
[2] C. E. Dunton, H. Q. Golder, H. E. G. Stripp, D. J. Henkel, D. A. Brown, D. L. Bartlett, F. L. Cassel, D. J. Palmer, D. J. Ayres, and R. F. Bonny, ICE Proceedings: Engineering Divisions **5**, 316 (1956).
[3] S. Marello, N. Lenoir, G. Viggiani, P. Bésuelle, J. Desrues, and M. Di Michiel, in *Proceedings of the International Workshop on X-Ray CT for Geomaterials, Kumamtoto, 2003* (Balkema/Taylor & Francis Group, London, 2004), pp. 139–146.
[4] H. J. Tillemans and H. J. Herrmann, Physica (Amsterdam) **217A**, 261 (1995).
[5] D. G. Fredlund and H. Rahardjo, *Soil Mechanics for Unsaturated Soils* (Wiley-IEEE, New York, 1993).
[6] J. K. Mitchell and K. Soga, *Fundamentals of Soil Behavior* (John Wiley & Sons, New York, 2005).
[7] M. R. Cunningham, A. Ridley, K. Dineen, and J. Burland, Geotechnique **53**, 183 (2003).
[8] M. Scheel, R. Seemann, M. Brinkmann, M. Di Michiel, A. Sheppard, B. Breidenbach, and S. Herminghaus, Nat. Mater. **7**, 189 (2008).
[9] T. Van Asch, J. Buma, and L. Van Beek, Geomorphology **30**, 25 (1999).
[10] R. Turton, Powder Technol. **181**, 186 (2008).
[11] H. Cetin, Turk. J. Eng. Environ. Sci. **23**, 465 (1999).
[12] Y. Higo, F. Oka, S. Kimoto, T. Sanagawa, and Y. Matsushima, *Advances in Bifurcation and Degradation*

in Geomaterials, Springer Series in Geomechanics and Geoengineering Vol. 11 (Springer Netherlands, New York, 2011), pp. 37–43.
[13] J. A. Dijksman and M. van Hecke, Soft Matter **6**, 2901 (2010).
[14] M. Jean, Comput. Methods Appl. Mech. Eng. **177**, 235 (1999).
[15] L. Brendel, T. Unger, and D. E. Wolf, *The Physics of Granular Media* (Wiley-VCH, Weinheim, 2004), pp. 325–343.
[16] D. Kadau, G. Bartels, L. Brendel, and D. E. Wolf, Phase Transit. **76**, 315 (2003).
[17] D. Kadau, H. Herrmann, and J. Andrade, Jr., Eur. Phys. J. E **30**, 275 (2009).
[18] A. Taboada, N. Estrada, and F. Radjaï, Phys. Rev. Lett. **97**, 098302 (2006).
[19] C. D. Willett, M. J. Adams, S. A. Johnson, and J. P. K. Seville, Langmuir **16**, 9396 (2000).
[20] S. Herminghaus, Adv. Phys. **54**, 221 (2005).
[21] S. Ulrich, T. Aspelmeier, A. Zippelius, K. Roeller, A. Fingerle, and S. Herminghaus, Phys. Rev. E **80**, 031306 (2009).
[22] R. Seemann, W. Mönch, and S. Herminghaus, Europhys. Lett. **55**, 698 (2001).
[23] L. Scholtès, P.-Y. Hicher, F. Nicot, B. Chareyre, and F. Darve, Int. J. Numer. Anal. Meth. Geomech. **33**, 1289 (2009).
[24] M. Scheel, R. Seemann, M. Brinkmann, M. D. Michiel, A. Sheppard, and S. Herminghaus, J. Phys. Condens. Matter **20**, 494 236 (2008).
[25] M. Kohonen, D. Geromichalos, M. Scheel, C. Schier, and S. Herminghaus, Physica (Amsterdam) **339A**, 7 (2004).
[26] See Supplemental Material at http://link.aps.org/supplemental/10.1103/PhysRevLett.109.248001 for the discrete equivalent of Eq. (2) which is given by Eq. (1).
[27] C. S. Campbell, J. Fluid Mech. **348**, 85 (1997).
[28] A. Ries, D. E. Wolf, and T. Unger, Phys. Rev. E **76**, 051301 (2007).
[29] P. Jop, Y. Forterre, and O. Pouliquen, Nature (London) **441**, 727 (2006).